S. Varcin, M. Fournier, J.M. Teissier[1] **ODN 1018**

DEP engineering, Saint-Martin-d'Hères, France

A 500 M LENGTH TEST STAND FOR ANALYSIS AND CHARACTERIZATION OF ELASTIC BEHAVIOR OF FIBER AND WIRE ROPES

Summary

It is admitted that a rope behaves like a spring-damper system so its behavior is completely determined by its stiffness k and its damping coefficient c.

The determination of k is usually done by pulling on a rope sample with a certain amount of force and by measuring the corresponding elongation. For short samples, as only a small amount of elongation is expected to be measured, measurement must be very accurate as a small error can lead to a significant variation of k. Instead, the relative error decreases drastically as the sample length increases. Besides, such a test cannot be used to determine the value of c.

Another method consists in hanging a mass to the rope sample, add a pre-stress and release it making the load oscillate as a mass-spring-damper system [1]. As for the force-elongation method, the longer the sample and the more accurate the measurements.

This method, called "dynamic method", has been implemented in a 500 m depth shaft in ANDRA CMHM underground laboratory, France. Different types of ropes have been tested: wire ropes and fiber ropes with different compositions and diameters. Different lengths have been tested as well, from 15 to 475 m. The goal of these tests was primarily to evaluate the test stand capabilities, not to determine ropes characteristics.

The results abide by what was expected, which highlights the relevancy of this method. On the other hand, limitations of the test bench have been identified, among which the softness of the bench itself, which is likely to disrupt the measurements. Some criteria are discussed in order to avoid such pitfalls. Besides, discrepancies between the spring-damper theory and the test data remain unexplained. Further studies to resolve these anomalies are discussed.

Keywords: wire rope, fiber rope, stiffness, damping, elasticity.

1 Characterization of the rope elastic behavior

It is widely admitted that ropes have an almost linear force-elongation relationship characterized by a stiffness coefficient k [2]. Usually, the rope elasticity is expressed as a Young's Modulus E, which allows to compare ropes with different diameters or compositions. E and k are linked by the following relation:

$$E = \frac{kL}{S}$$

[1] Email: dep@dep-engineering.fr

where L is the length of the sample and S the cross-section of the rope.

The stiffness can easily be evaluated during static tests by measuring the rope elongation versus the line-pull in the rope (static method). Especially if the rope sample is short, the measurements must be very accurate and the stiffness of test bench should be considered as well as the possible slippage of the connectors. The measured stiffness also depends on the rope "bedding-in". The graphs below present the results of such measurements performed with the DEP's Twist/Torque test stand.

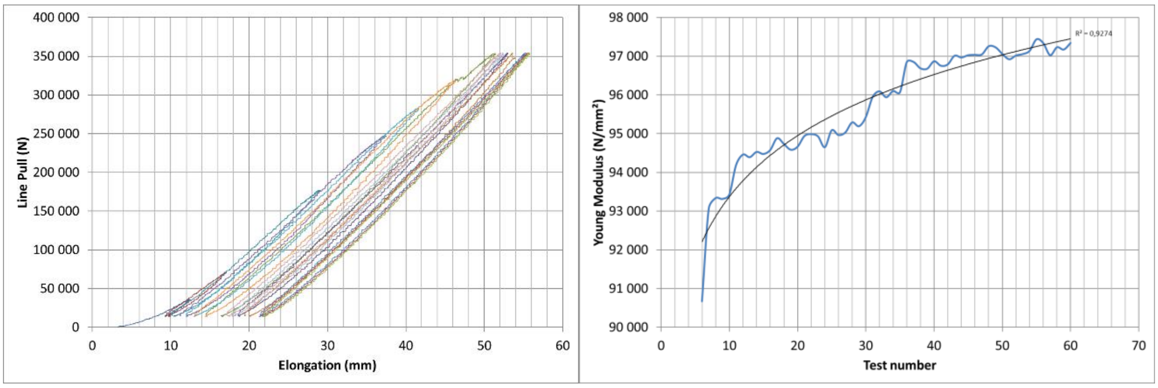

Figure 1: rope tensile test with multiple cycles (left); stiffness measured at each cycle (right)

Besides, dynamic tests have shown that ropes present damping when elongated at significant velocities. It is admitted that the damping is proportional to the elongation velocity [2]. As a consequence, the damping can be completely characterized by a single coefficient c.

The elastic force F is proportional to the elongation x: $F = kx$. Imagine the rope is cut into n identical parts, whose stiffness is k' and its length L' ($L' = \frac{L}{n}$). Under force F, each part is submitted to the same elongation x', hence $x = nx'$. Then $\frac{F}{k} = n\frac{F}{k'}$, then $k = \frac{k'}{n}$. Hence $kL = k'\frac{L}{n} = k'L'$. So, for a given rope, kL is constant.

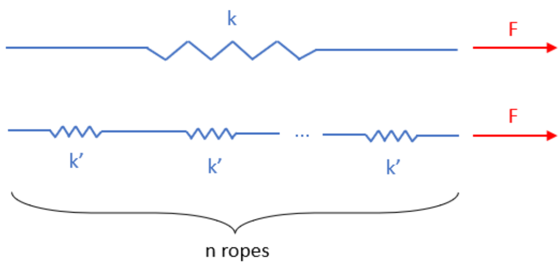

The viscous friction force is proportional to the elongation velocity: $F = cv$. Imagine the rope is cut into n identical parts, whose damping coefficient is c' and its length L' ($L' = \frac{L}{n}$). Under force F, each part is submitted to the same elongation velocity v', hence $v = nv'$. Then $\frac{F}{c} = n\frac{F}{c'}$, then $c = \frac{c'}{n}$. Hence $cL = c'\frac{L}{n} = c'L'$. So, for a given rope, cL is constant.

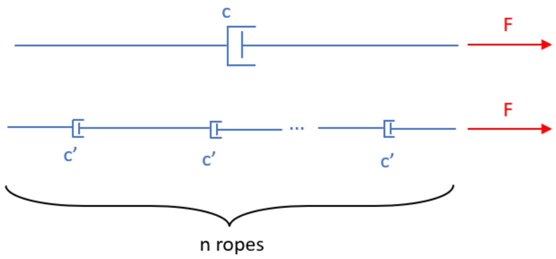

Thus, a sample of rope on which a load is hanged behaves like a mass-spring-damper system.

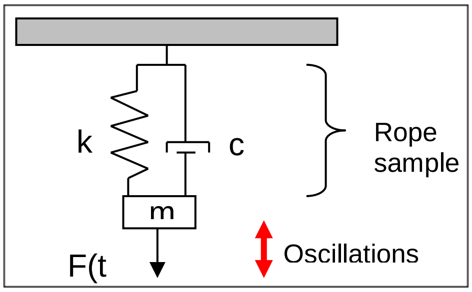

Figure 2: spring-damper model

Then it is possible to determine c and k making the load oscillate. Two dynamic methods can be considered:

- The free oscillations method, in which the load is initially pulled down and suddenly released
- The driven oscillations method, in which the load is shaken at a constant frequency

1.1 Free oscillations method

This method is well-known and has already been investigated [1, 2, 3]. When the load oscillates freely, its motion is ruled by the following equation.

$$m\frac{d^2x}{dt^2} + c\frac{dx}{dt} + kx = 0$$

where m is the load's mass, c and k the damping and stiffness coefficients of the sample and x the position of the load (as a function of time).

The solution of this equation is

$$a(t) = \alpha e^{-\lambda t}\cos(\omega t + \varphi)$$

where a is the load's acceleration ($a(t) = \frac{d^2x(t)}{dt^2}$), λ the exponential decay factor and ω the angular frequency. The following graph shows the acceleration as a function of time.

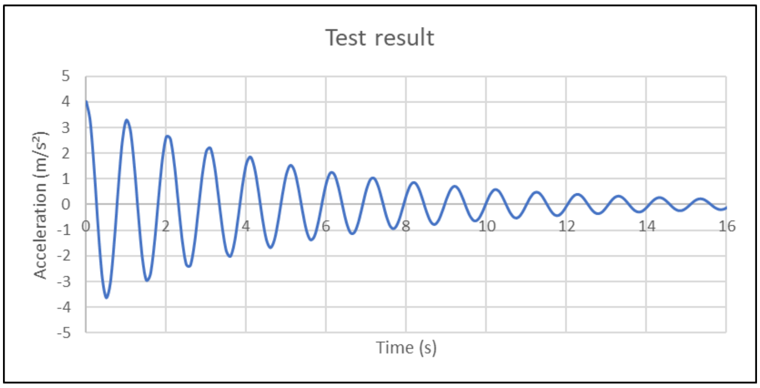

Figure 3: acceleration of the load over time

Two methods can be used to identify parameters λ and ω from the acceleration curve. The first one consists in calculating an exponential regression from all extrema, which allows to find λ. ω is calculated by measuring the time interval over a certain number of oscillations divided by this number.

On the following, example, we find that λ = 0.188 s-1 and ω = 2π/T = 6.14 s-1.

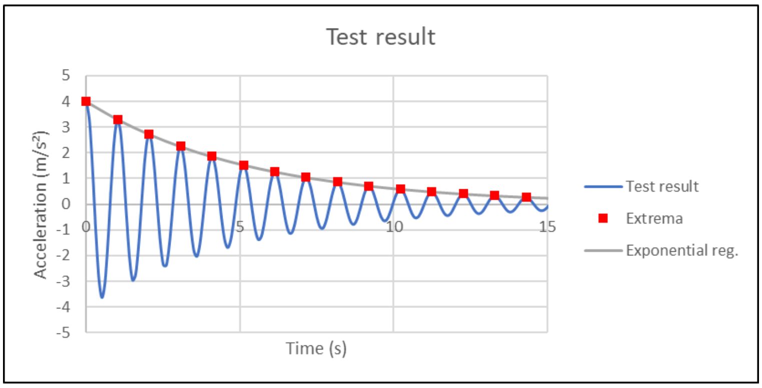

Figure 4: identification of parameters λ and ω

The second is to calculate directly a regression in the form of $\alpha e^{-\lambda t}\cos(\omega t + \varphi)$. On the following graph, the orange curve is the regression of the test curve (blue). We find the same values for λ and ω as with the first method.

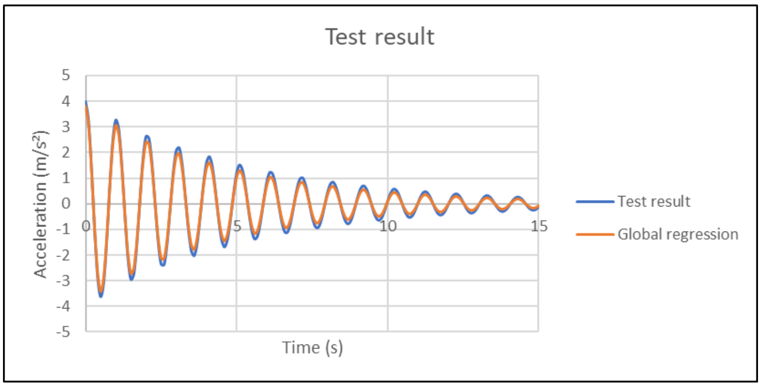

Figure 5: regression on the test curve

Then c and k can be obtained using the following formulas:

$$c = 2m\lambda$$

$$k = m(\omega^2 + \lambda^2)$$

As kL and cL are constant, once known for one length, k and c can be calculated for any length.

1.2 Driven oscillations method

This method consists in making the load vibrate with a sinusoidal force at a certain frequency. Measuring the amplitude of the acceleration at different (at least two) frequencies allows to determine c and k.

A specific test stand has been built in order to evaluate this method. The tested rope is attached to the top of a mast. A counterweight including a rotating machinery with off-center masses is suspended to the rope. The speed revolution of the machinery is adjusted in order to generate the vibration of the rope.

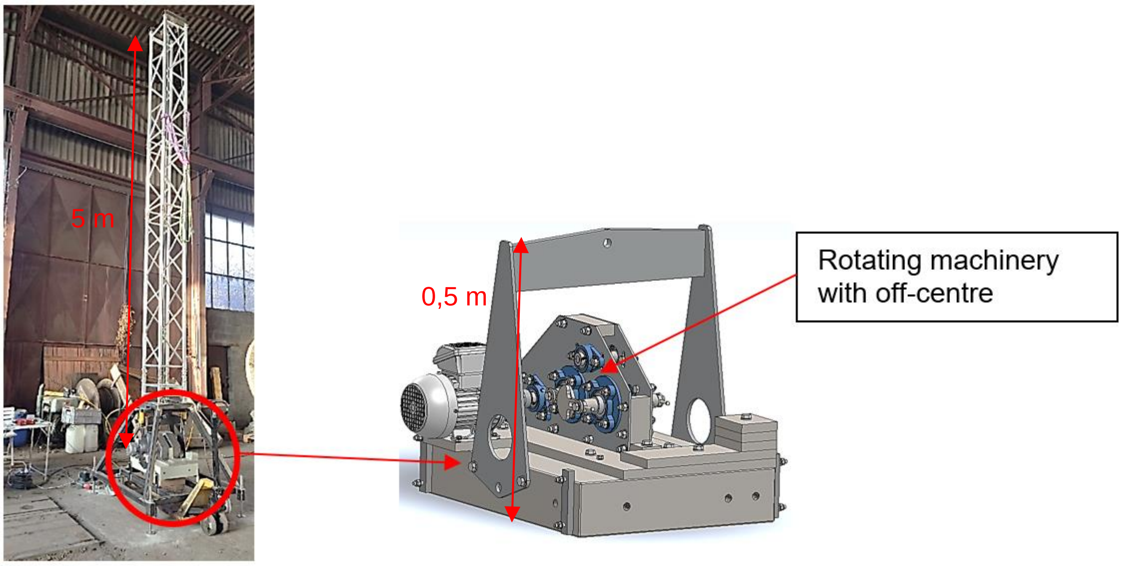

Figure 6: driven oscillations test stand

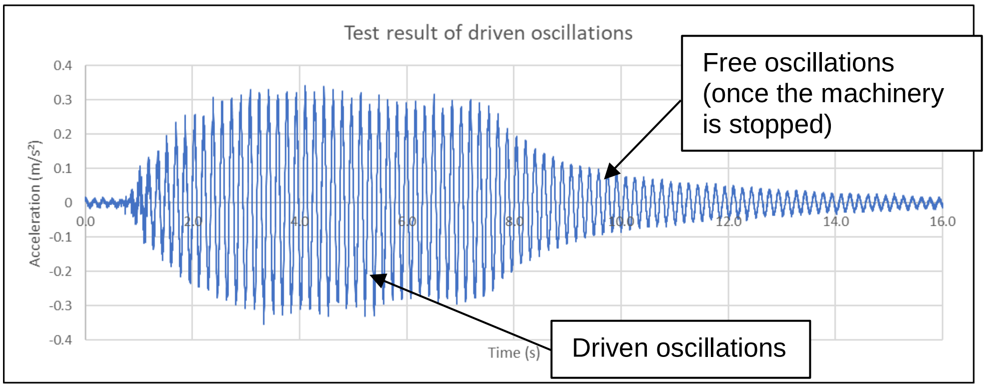

Figure 7: acceleration of the load for a driven oscillations test

According to the few samples tested with both methods, it seems that the driven oscillation method and the free oscillation method give identical results.

This method has not yet been implemented in the 500 m shaft, because it requires an exciter able to provide a significant amplitude at a very low frequency. The rotating machinery presented above is not able to do so but developments are ongoing.

1.3 Understanding the rope behavior

It is admitted that the damping is due to the friction between wires. If this friction follows the Coulomb's law, the resultant force should not be proportional to the velocity but only on its sign. However, simulations have shown that with Coulomb friction the decay is linear (Figure **8**) and not exponential, as observed in the tests.

A possible path for explaining the actual exponential decay on the basis of friction forces could be find in the transition between the static friction coefficient and the kinetic one. At this point, we do not have any other explanation on how the damping may depend on the velocity.

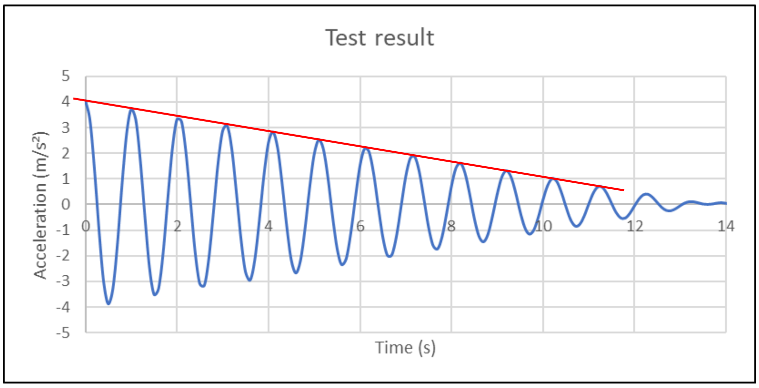

Figure 8: result of a simulation with Coulomb friction force

Besides, we can mention the "critical damping", damping value above which the load goes back to its equilibrium position with no oscillation. It takes the following value: $c_{crit} = 2\sqrt{km}$. The ratio between the damping and the critical damping is commonly used in seismic calculations as it gives the type of response (underdamped or overdamped) the rope will provide if excited by seismic waves: $\zeta = \frac{c}{c_{crit}}$. Some laws and standards ruling the design of structures for seism resistance consider a damping of 5% for the critical damping.

1.4 Appreciation of the rope behavior

When attending tests of ropes with different stiffnesses, we can wrongly conclude that the softest rope is more damped than the stiffest whereas they both have the same damping. The example below shows two ropes with a different stiffness but the exact same damping.

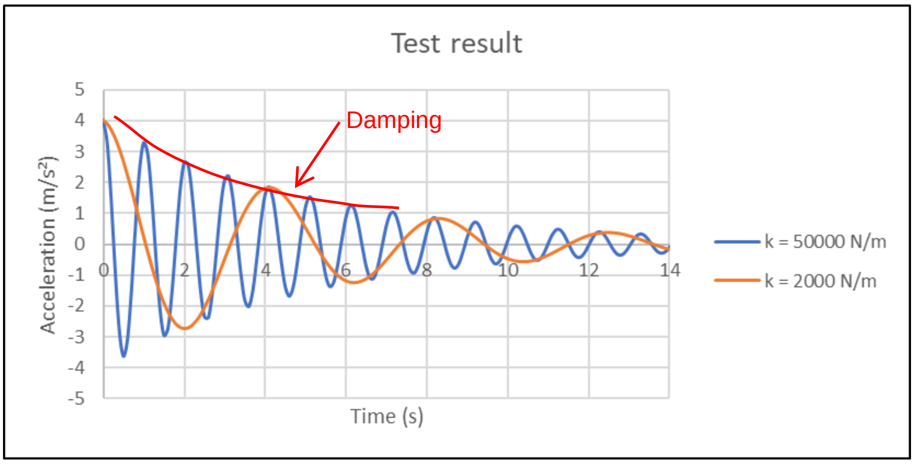

Figure 9: comparison of two ropes responses. Both samples have the same damping.

With the rope whose stiffness is the highest, we would see the load oscillating quickly with a small decrease in amplitude between two consecutive oscillations. Conversely, we would see the other rope oscillating slowly with a large decrease in amplitude between two consecutive oscillations. However, which matters is not the decrease in amplitude from one oscillation to another but the decrease over a certain period of time. From the beginning to 3 s, both amplitudes have been divided by around 3 so both ropes have the same damping.

2 Test stand

Tests are conducted in ANDRA CMHM underground laboratory, France. The site includes two shafts (called “PA” and “PX”), which go 500 m deep. The rope sample is hanged under one of the elevators of the PX shaft. The cabin is suspended on parachute ropes. Those parachute ropes are hanged on a steel structure at the top of the shaft. This structure, as well as the parachutes ropes, are supposed to have a stiffness significantly higher than the sample tested. This point is discussed later. At the other end of the rope, a load of 400 kg is attached. An additional tension of about 200 kg is applied by means of a manual winch. This additional tension is then suddenly released by means of an electromagnet, which makes the load oscillate.

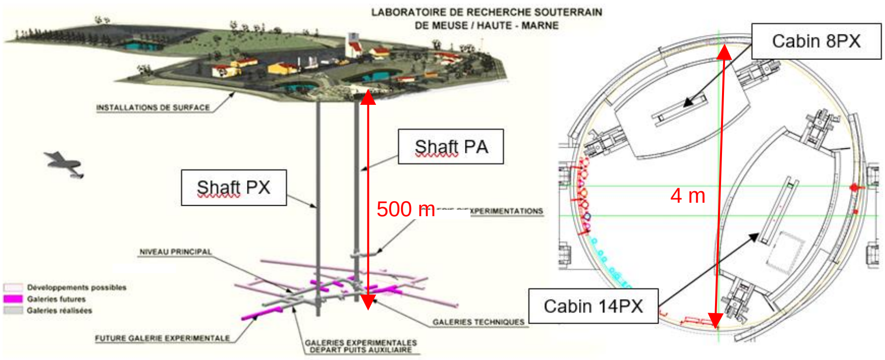

Figure 10: drawing of ANDRA Laboratory (left). Plan of PX shaft (right).

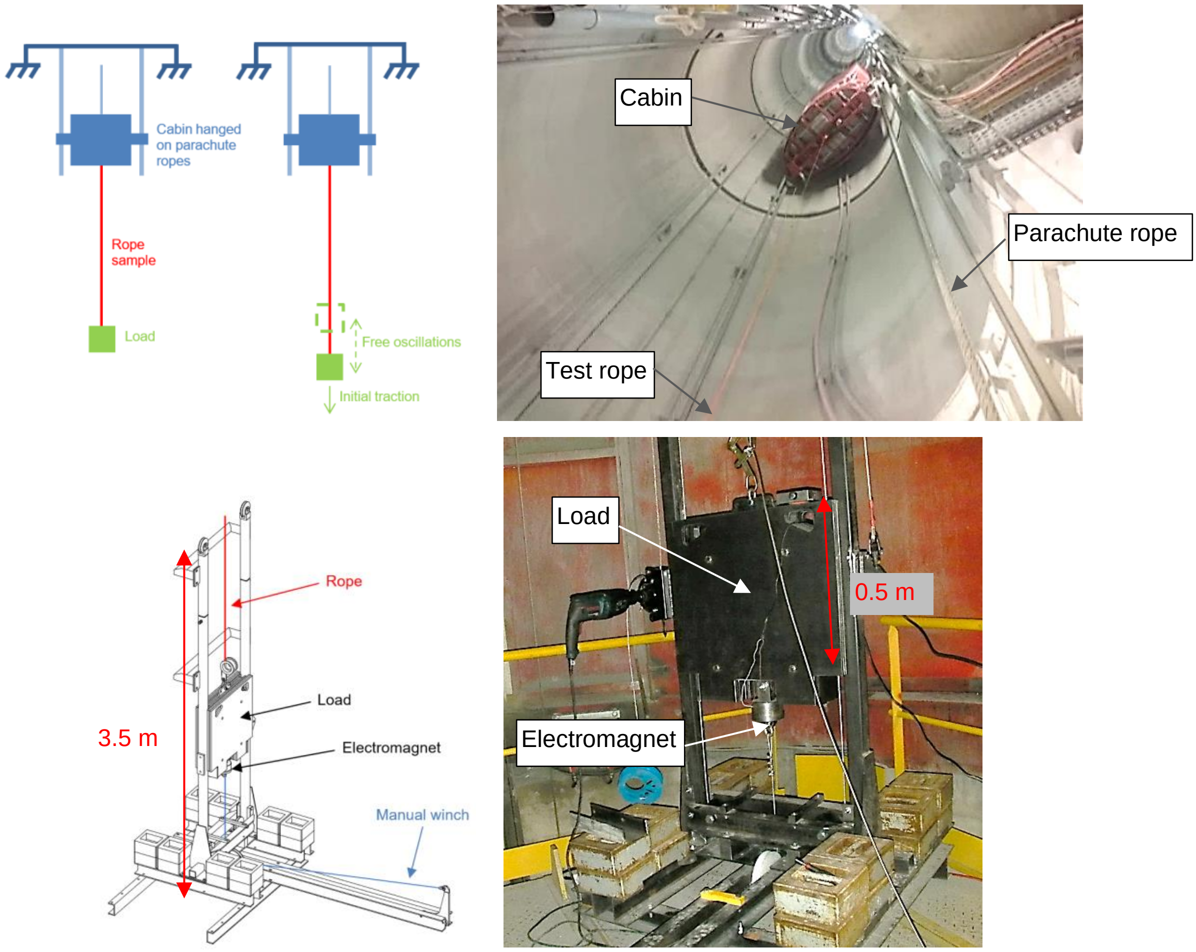

Figure 11: drawings and photos of the test stand

3 Stiffness of the test stand

The theory exposed in §1.1 assumes that the upper anchor of the rope sample is perfectly immobile. In reality, the cabin is not strongly anchored to the shaft but hanged on parachute ropes instead.

The total parachute ropes stiffness has been estimated at k = 212 000/L (kN/m), where L is the distance between the cabin and the parachute ropes anchor.

The top structure also has its own stiffness. It has been estimated at 83 000 kN/m.

Then, when short samples are tested, L is high so the stiffness of the parachute ropes is low and the cabin is likely to move during the test, disrupting the measurements. When samples of 500 m are tested, the parachute ropes are very stiff (because very short) but the anchorage stiffness is still limited by the top structure.

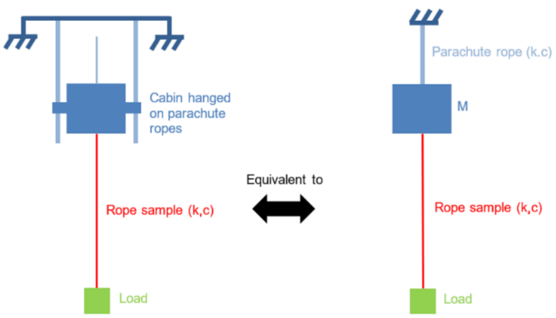

Figure 12: the test stand behaves like two mass-spring-damper systems in series

The following graphs show how the measurements of kL and cL are disrupted because of the stand softness.

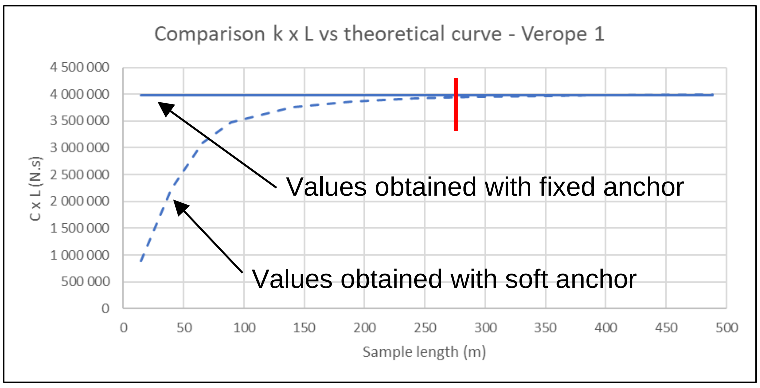

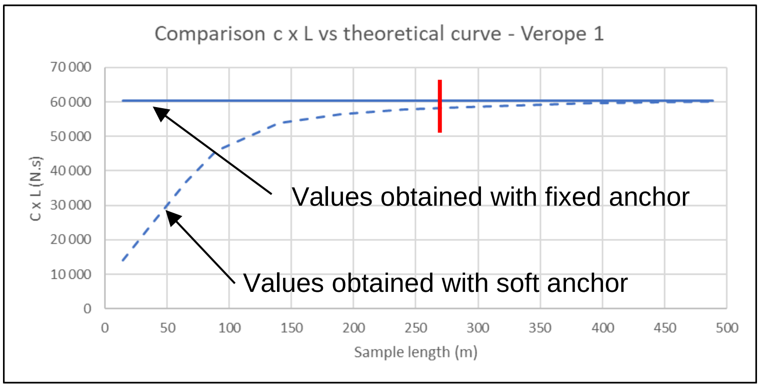

Figure 13: values of kL and cL measured if the anchor is fixed (solid line) or soft (dotted line)

For short samples, the error can be significant. Simulations have shown that the ratio between the sample rope stiffness and the parachute rope stiffness should be less than around 1% in order for the error on kL to be less than 2% (this limit is shown by a red stroke on figure Figure **13**).

The following diagram shows, as an example, the values of k and c for a wire rope, as well as the theoretical values calculated from different data points (corresponding to different stiffness ratios which correspond to different sample lengths).

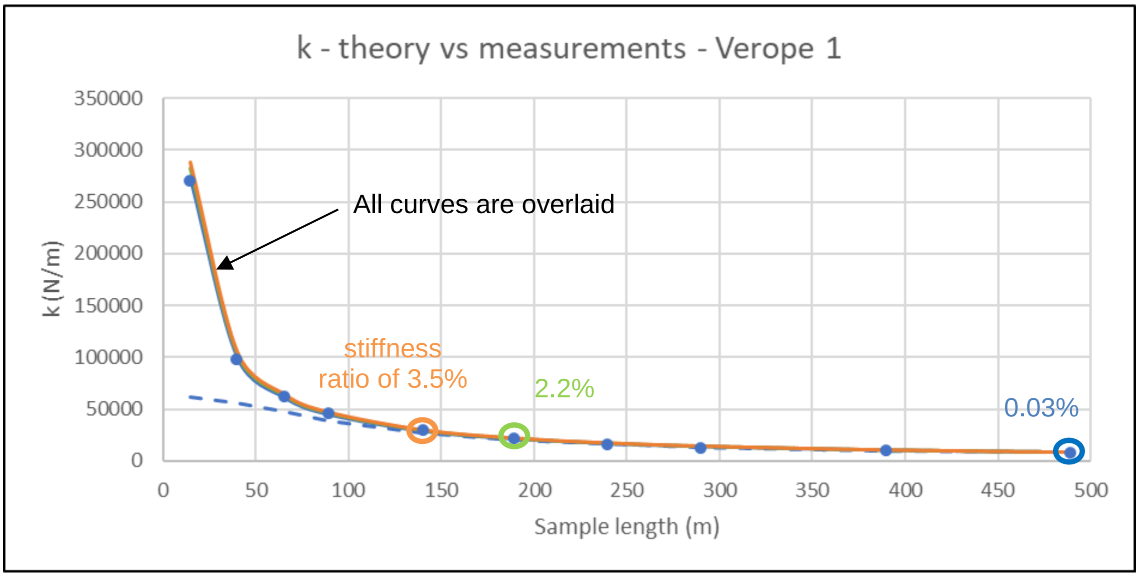

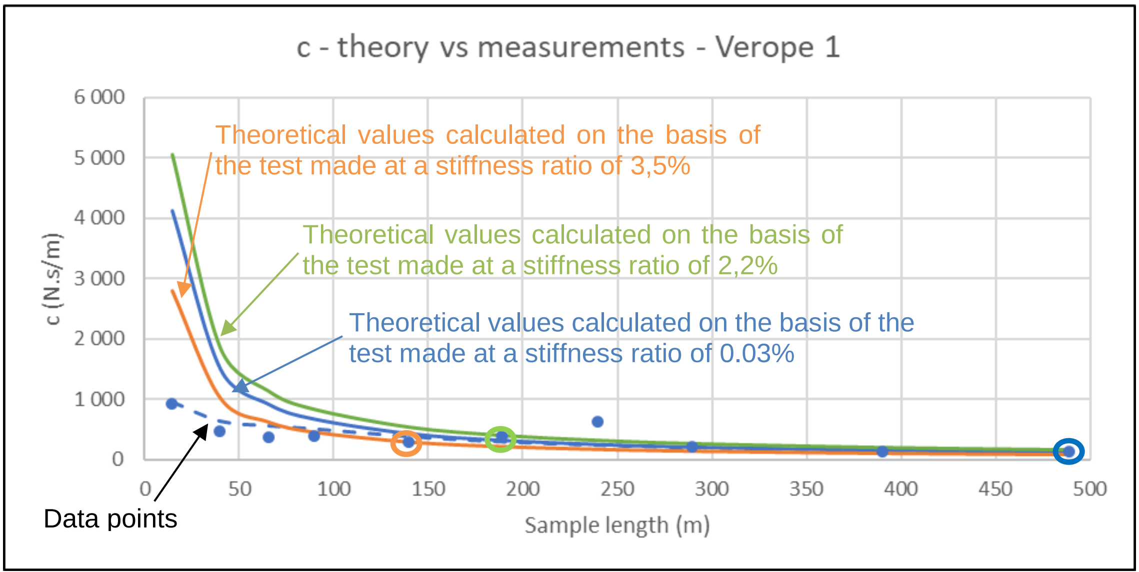

Figure 14: theoretical values of k and c assuming kL and cL are constant, calculated from different data points (corresponding to different stiffness ratios).

The lack of stiffness of the test stand creates significant differences that can be avoided by using data got during test performed with an appropriate (smaller) stiffness ratio.

The damping factor c, is much more sensitive to the stiffness ratio during the test than the stiffness k.

The accuracy of the measurements performed with that test stand is discussed on §5.2.

4 Tests performed

4.1 Ropes tested

The following table lists the ropes that have been tested and their main characteristics.

Designation / ID	**Type**	**Nominal diameter** (mm)	**Breaking strength** (kN)	**Linear mass** (kg/m)	**Cross-section** (mm²)	**Filling factor**
Rotation-resistant **Verope 1**	steel	8	55	0.305	35.2	0.70
8-strand plasticized IWRC **Verope 2**	steel	8	58	0.288	33.4	0.66
Semi rotation-resistant **(19x7)**	steel	12	104	0.600	65.8	0.58
12-strand Braided Advanced fiber, Specific design **Yale Cordage 1**	HMPE	4.76 (3/16”)	26	0.015	?	?
12-strand Braided Standard fiber, Standard design **Yale Cordage 2**	HMPE	6.35 (1/4”)	29	0.022	?	?
6-strand wire-lay construction HMPE jacket **Whitehill**	Aramid	8	67	0.060	?	?
6-strand wire-lay construction HMPE jacket **Whitehill**	Aramid	14	205	0.152	?	?

Table 1: tested ropes

Verope 2 sample has been tested twice. The first test (Verope 2 - 1), which was implemented with no pre-stretching, can be considered as pre-stretching for the second test (Verope 2 - 2).

Fiber ropes have been pre-stretched before being tested.

The cross-section values are unknown for fiber ropes, so dealing with Young’s modulus might be confusing. Consequently, it is preferable to deal with the equivalent modulus $E_{eq} = kL/d^2$, where k is the rope’s stiffness, L its length and d its nominal diameter. E_{eq} is analog to the Young’s modulus but without depending on the cross-section. If the actual section S is known, then the relation between E_{eq} and E is $E = E_{eq}d^2/S$.

4.2 Measured stiffness

Concerning the stiffness, these tests have shown that:

- the dynamic method gives much better results than the static method, especially for short samples
- the stiffness (measured with the dynamic method) is not much affected by pre-stretching due to previous tests

The graph below shows the module measured with the static method for all ropes.

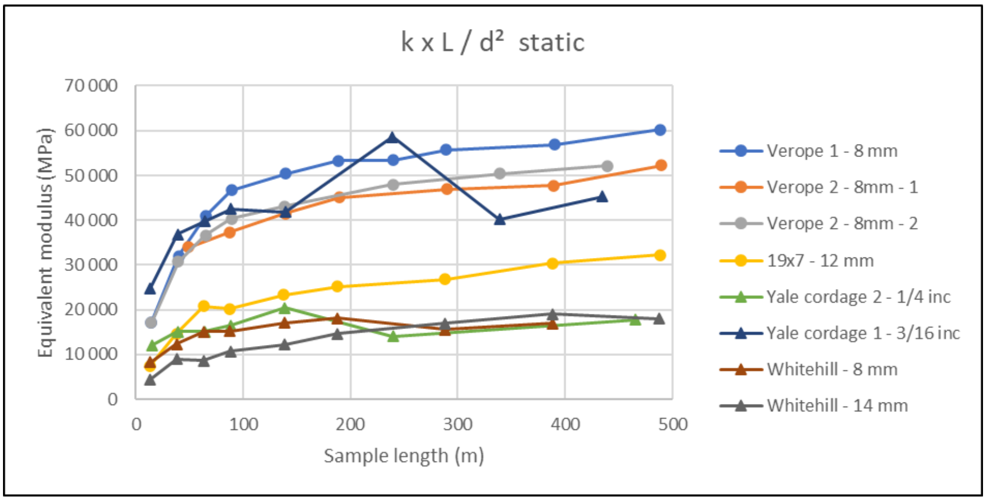

Figure 15: equivalent module obtained by the static method

The graph below shows the module measured with the dynamic method for all ropes.

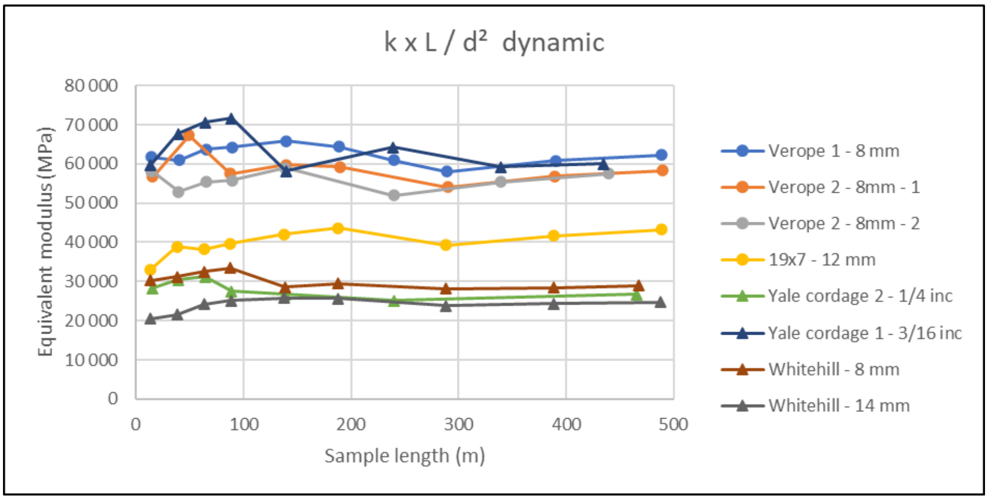

Figure 16: equivalent module obtained by the dynamic method

As we expect, the module is independent of the sample length. The small variations can be due to the limited accuracy of the measurements, especially for short samples.

The graph below shows the kL measured with the dynamic method for all ropes.

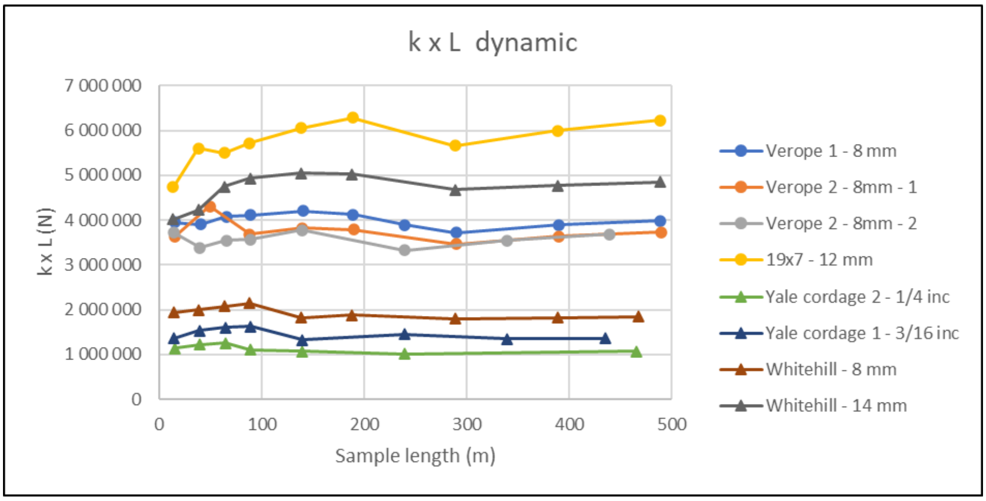

Figure 17: values of kL obtained by the dynamic method

4.3 Measured damping

4.3.1 Measurements from the test stand

The graph below shows the damping coefficient for all ropes.

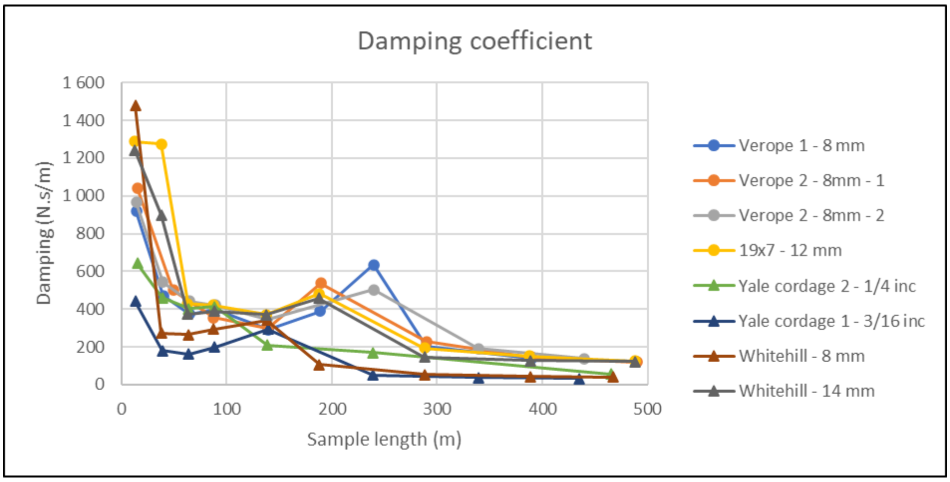

Figure 18: damping values of tested ropes

The graph below shows the cL for all ropes.

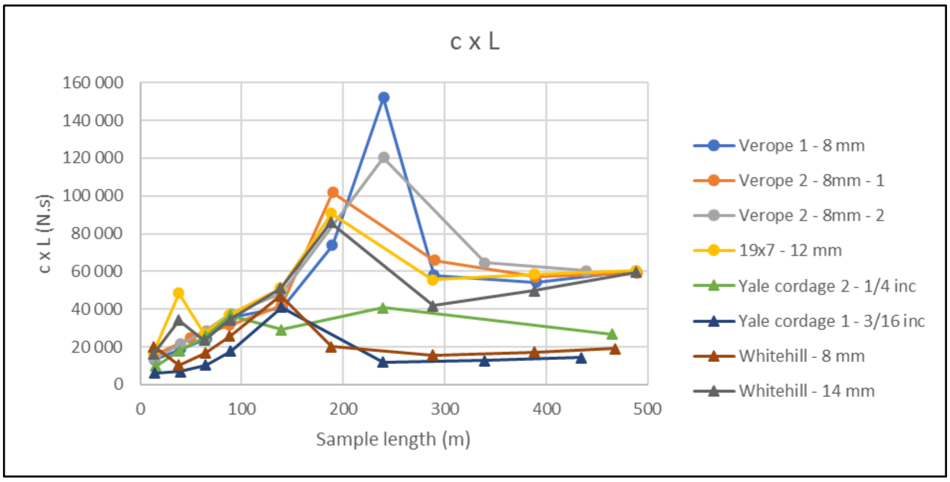

Figure 19: values of cL

All tests showed that cL is not independent from the rope's length, as we would expect. Moreover, we can notice that all result curves seem to follow the same pattern: for short samples, cL increases with L. For long samples, cL is almost constant. In between, surprisingly high values are reached. Here are two examples of the ropes tested.

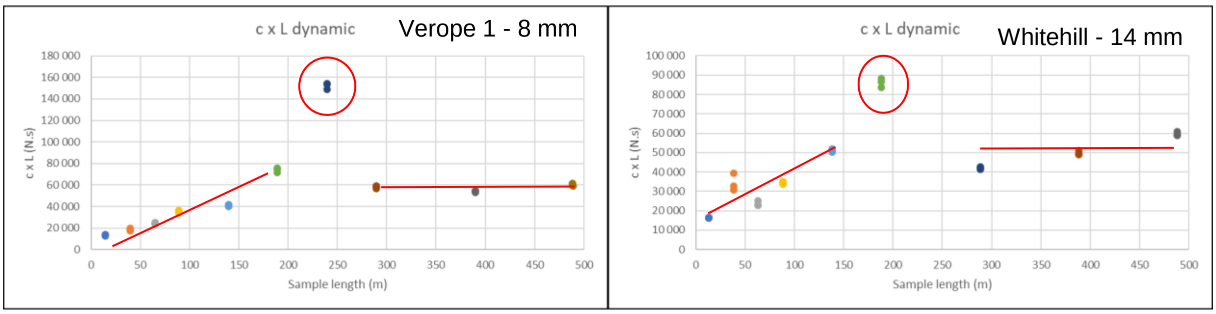

Figure 20: values of cL measured for two ropes

4.3.2 Other measurements

Other tests have been performed in the shaft using the Casar Turboplast 16 mm cabin's suspension ropes. Some tests, which have been implemented with new ropes in 2005-2006 during the construction of the laboratory, have been reproduced in 2022 with the same ropes.

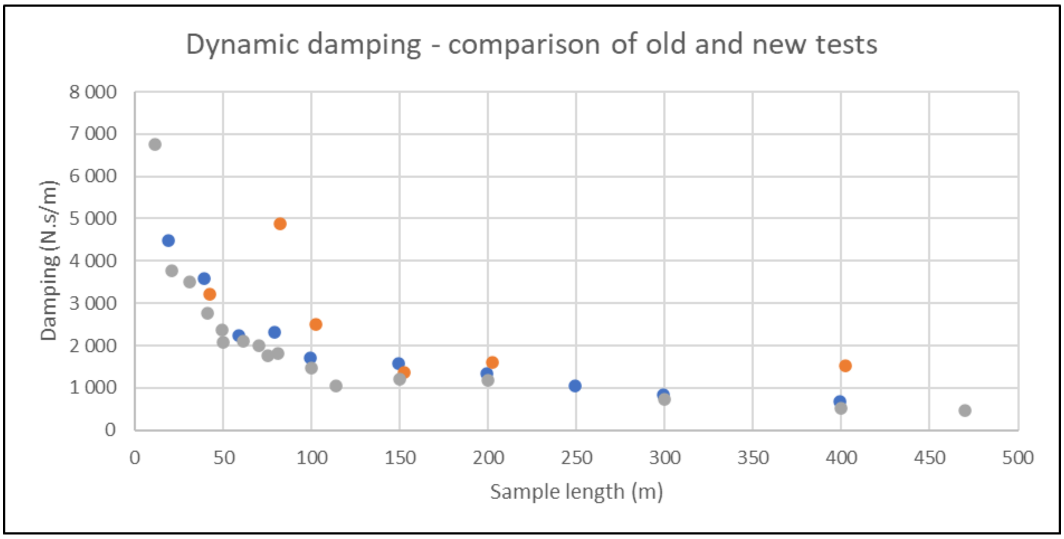

Figure 21: Damping measured on the elevator ropes in 2005 (grey) and 2023 (blue/orange).

One measurement has also been performed during the laboratory construction with a Casar Turboplast 44 mm rope, which was the suspension rope of the shaft boring equipment.

The diagram below summarizes all the results got with wire ropes.

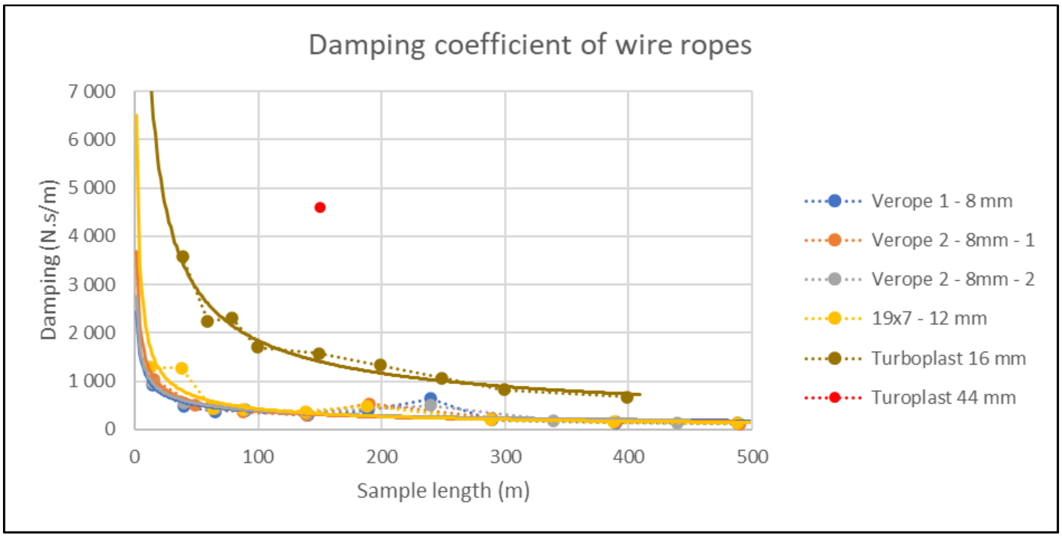

Figure 22: damping factor for wire ropes

5 Discussion about the results

5.1 Stiffness

Concerning the stiffness, it is surprising that kL is almost independent from the length, even for short lengths. Indeed, when the 1% ratio is not fulfilled, simulations show that the measurement of k should be disrupted too (see §3), which does not seem to be the case in our tests.

The diagram below shows the expected results considering the stiffness of the test stand and results of the measurements.

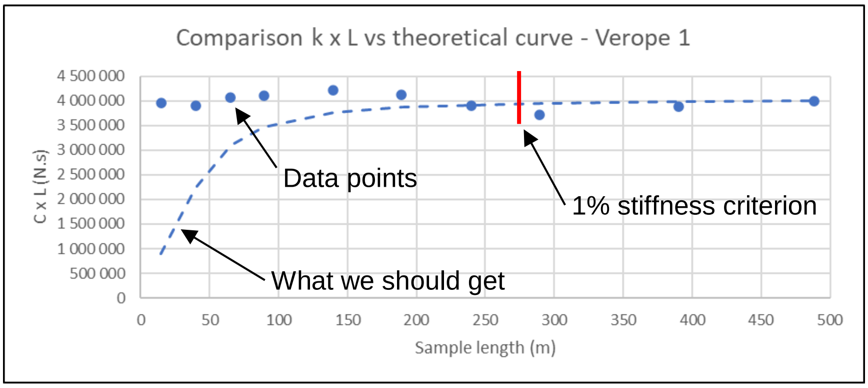

Figure 23: comparison between values of kL measured and simulation results

Works remain to be done to clarify that matter.

5.2 Damping – accuracy

Unexpected results are found for the damping. For short lengths the small values of cL can be explained by the softness of the anchor. For medium lengths, some values are incredibly high. Works remain to be done to explain such variations.

As explained in §3, the measurements can be considered as relevant only when the test rope stiffness is lower than 1% of the test stand stiffness.

On the following graph, vertical strokes show the length above which this condition is fulfilled.

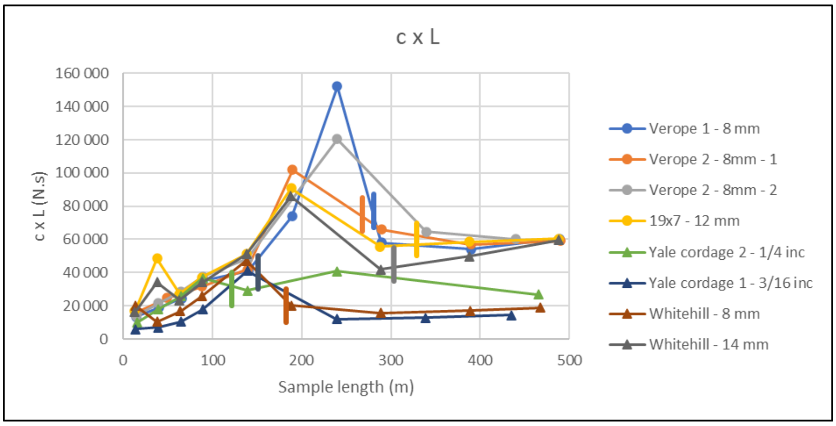

Figure 24: values of cL. For each rope the vertical stroke gives the 1% stiffness ratio.

We can see that, for all ropes, cL is almost constant above the stiffness criterion.

This disruption can be highlighted by integrating the measured acceleration twice, so that we get the load's displacement. The following graphs show the acceleration measured on a 15-meter sample and the same curve integrated twice (load's displacement).

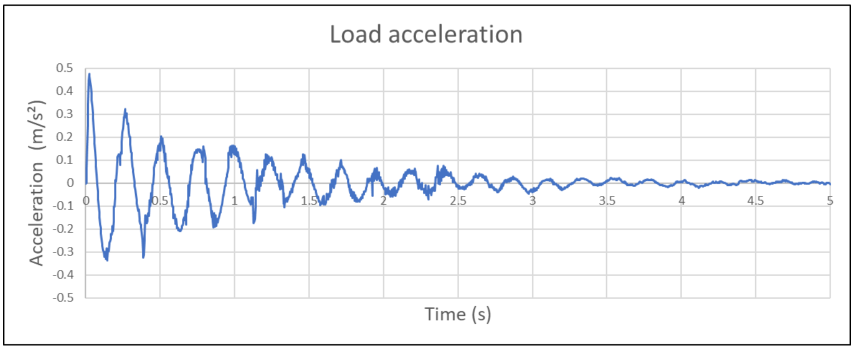

Figure 25: acceleration of the load measured during one of the tests

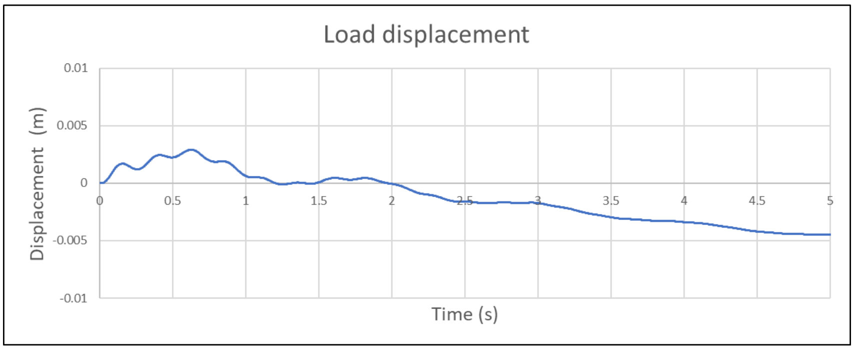

Figure 26: displacement of the load obtained by integrating the acceleration twice

The load's motion is far for being pseudo-periodic with exponential decay as we would expect. On the other hand, for long samples (small stiffness ratio) the behavior matches well with the theory.

The following curves show the velocity measured for different lengths of a rope. It confirms that, below a stiffness ratio of about 1%, the measured velocity is really consistent with the mathematical model.

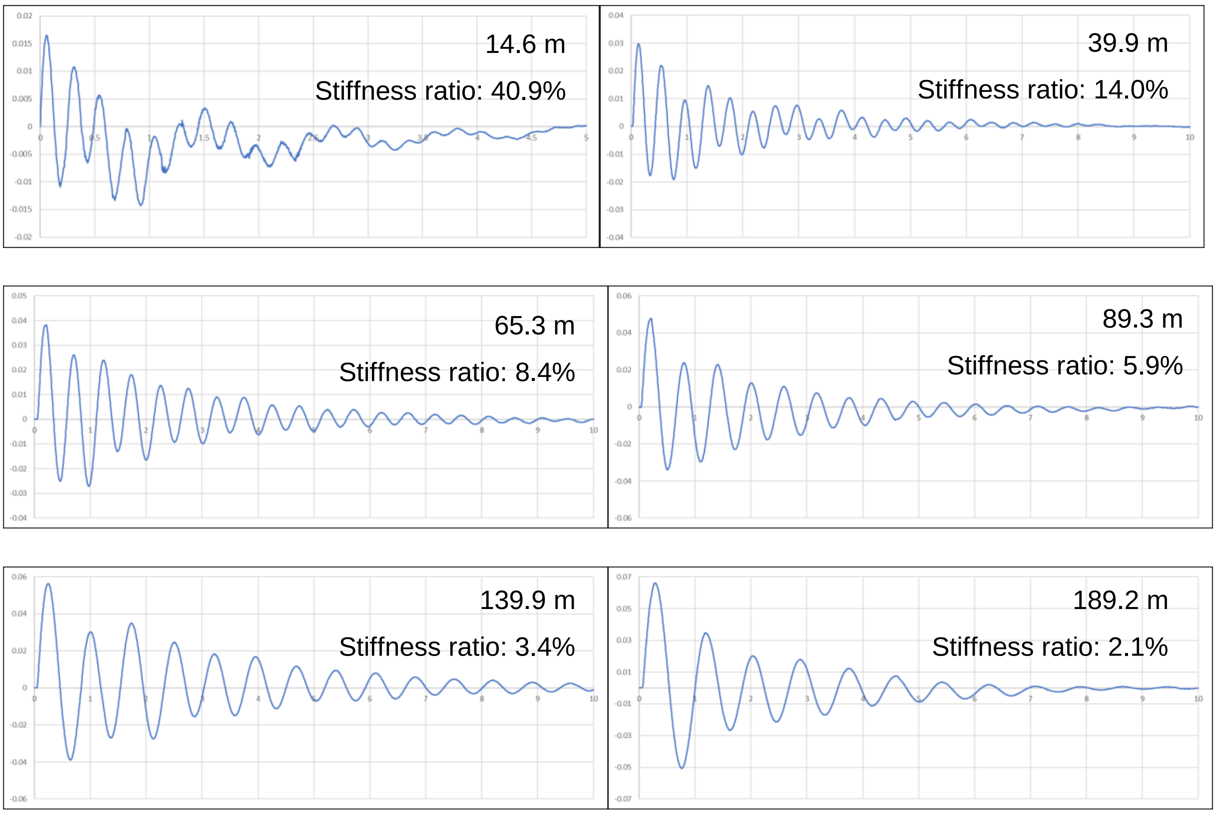

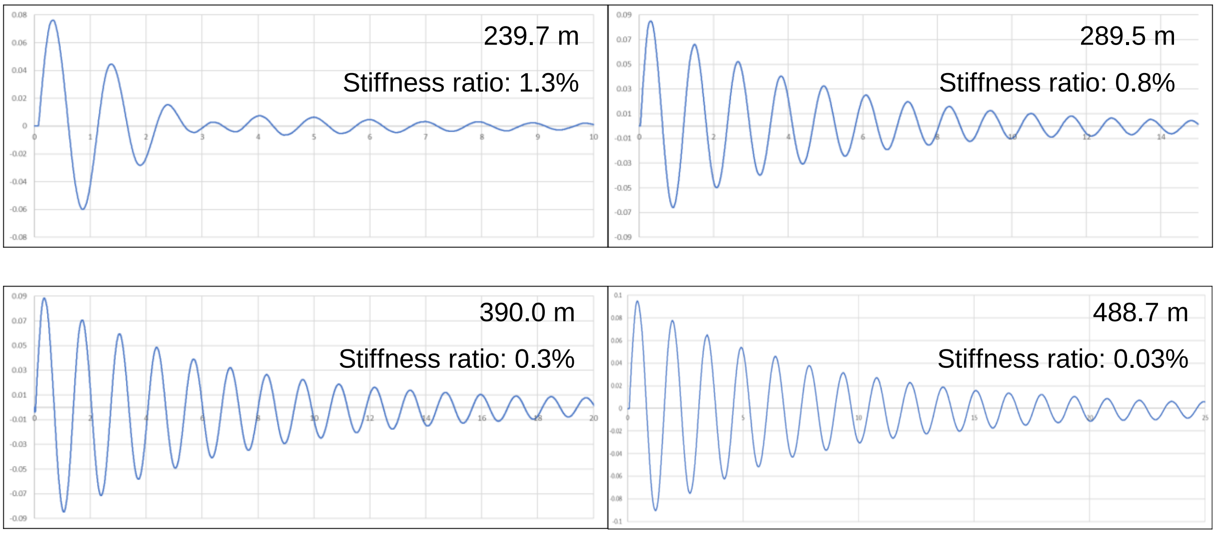

Figure 27: load velocity measured for different sample lengths for an 8 mm metallic rope

We can assume that the smaller the stiffness ratio is, the higher the accuracy will be.

Diagrams below compare the curves of c calculated on the basis of different stiffness ratios for some of the tested ropes.

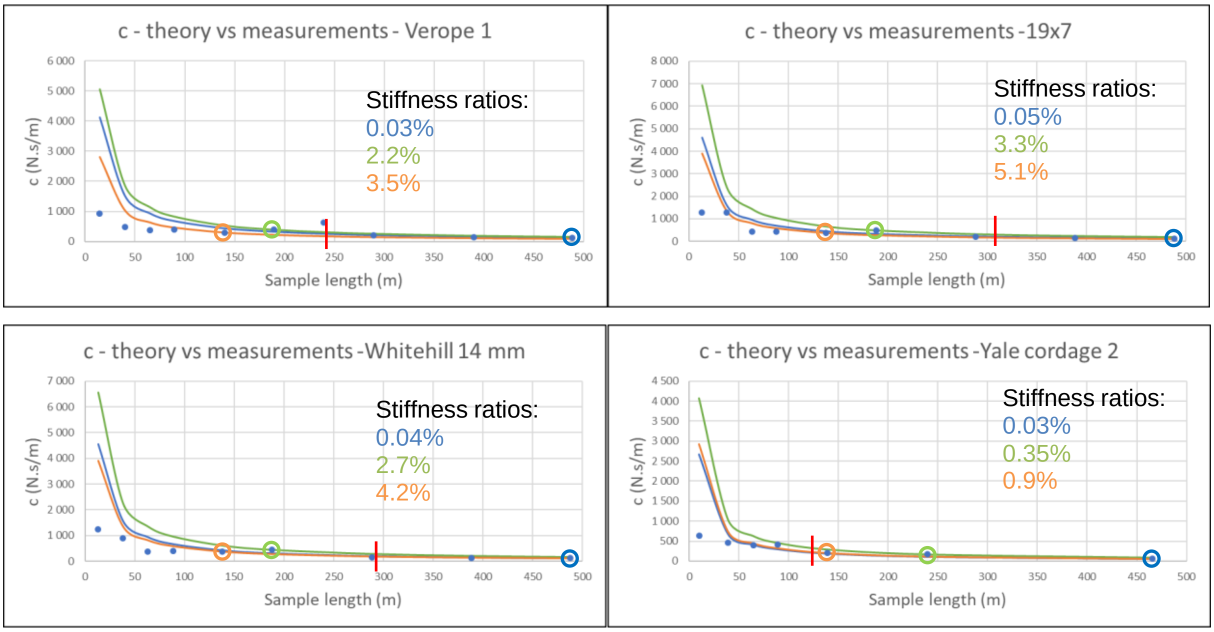

Figure 28: theoretical values of c assuming cL is constant calculated from different data points (corresponding to different stiffness ratios). Values of reference are circled with the corresponding color. The vertical stroke gives the 1% stiffness ratio

The diagrams above show that not only the stiffness ratio should be considered, but also the sample length. For the rope Yale Cordage 2 calculations on the basis of a stiffness ratio of 0,35% leads to an about 52% mistake for sample length of 10 m.

Both criteria should be considered as cumulative.

5.3 Damping – bedding-in influence

The results shown on figure Figure **21** are almost identical, which tends to show that the damping factor is not influenced so much by the bedding-in of the rope. Further tests will be conducted to confirm this assumption.

Results got with the two tests performed with rope Verope 2, tend to confirm this assumption.

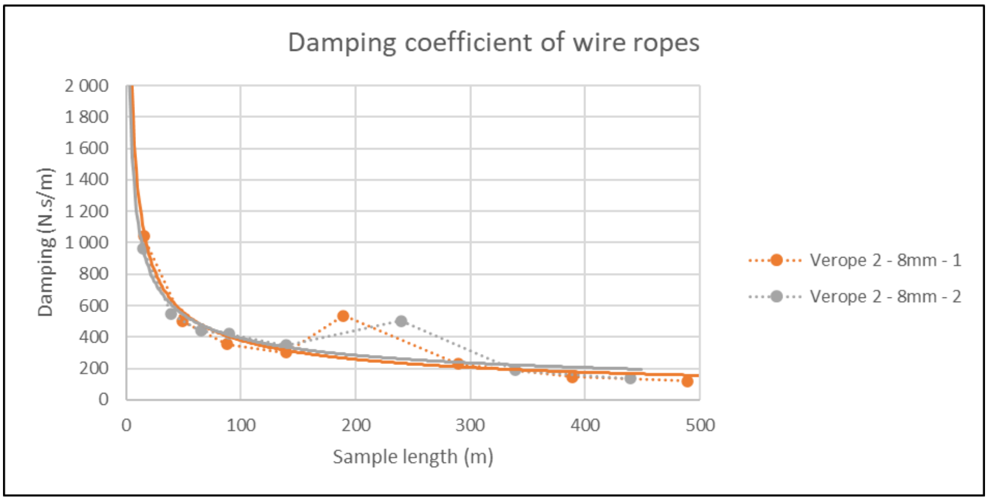

Figure 29: Damping coefficient of unstretched and stretched rope samples

5.4 Damping – diameter influence

The results got with wire ropes (see figure Figure **22**) show that the damping factor increases accordingly with the rope diameter.

The diagram below shows the same behavior for fiber ropes.

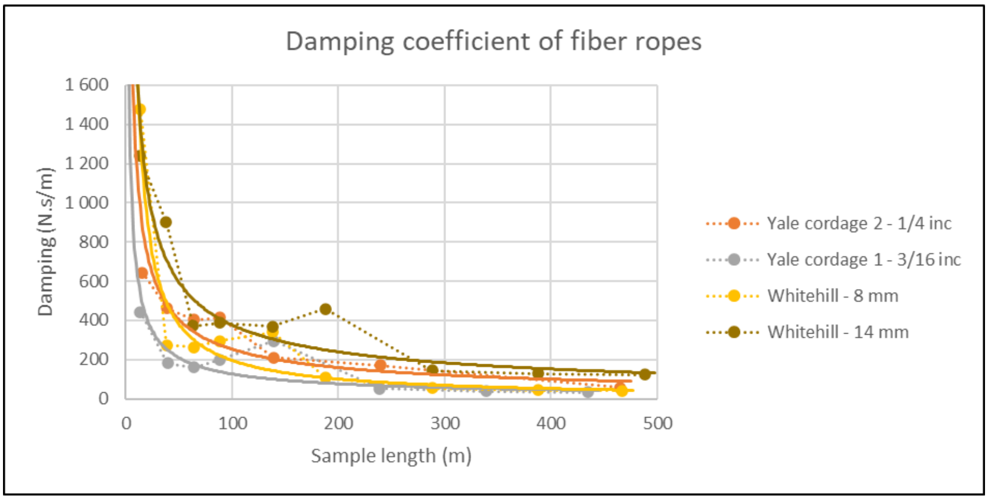

Figure 30: Damping factor for fiber ropes

5.5 Damping – analysis regarding critical damping

As presented in §1.3, the ratio between the damping and the critical damping ($\zeta = \frac{c}{c_{crit}}$) is commonly used in seismic calculations. We may think that this ratio depends on the safety factor, because even if c is independent of the mass, c_{crit} depends on the mass, i.e. on the safety factor. However, curves of figure Figure **31** tend to show that this ratio is not dependent on the rope safety factor.

The diagram below shows this ratio for some of the tested ropes. We have considered the measurements, and also data calculated on the basis of the assumption presented in §5.2.

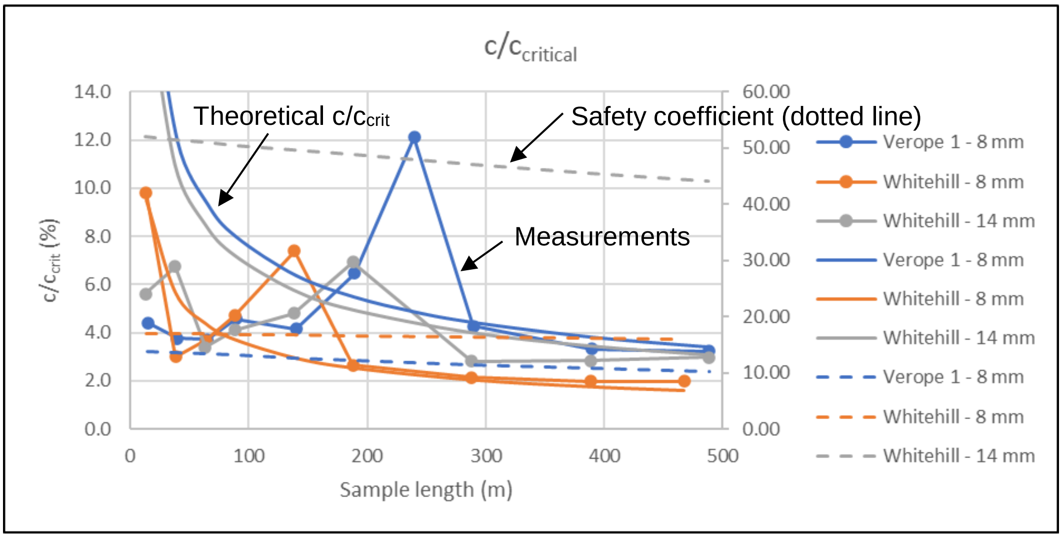

Figure 31: variation of $c/c_{critical}$ for three ropes

5.6 Damping – fiber ropes / wire ropes comparison

An accurate comparison between fiber ropes and wire ropes would require much more experimentations. The damping factor seems to be dependent on the rope diameter, and, for the same diameter, fiber ropes (at least those so far tested) do not have the same stiffness as the wire ropes.

As a preliminary investigation, we can compare two wire/fiber ropes with similar stiffnesses, and two wire/fiber ropes with the same diameter. The diagrams below show the results got.

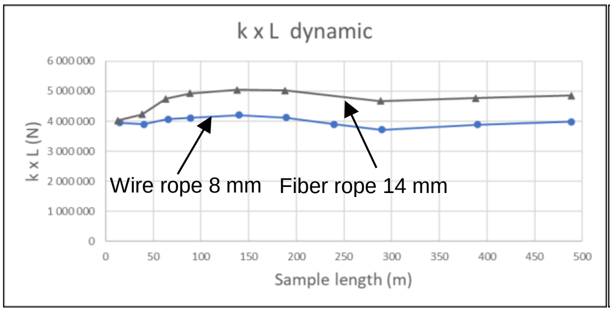

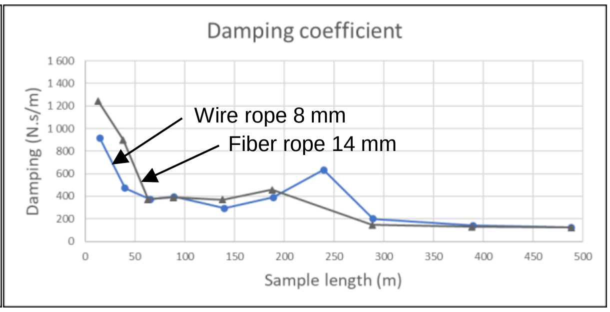

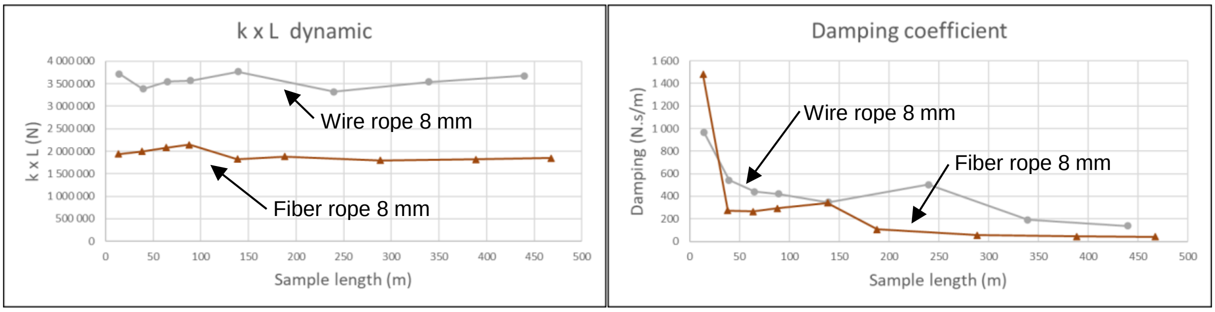

Figure 32: comparisons of damping and stiffness between wire and fiber ropes

The results above tend to show that fiber ropes have a slightly smaller damping factor than wire ropes.

6 Test stand capabilities

This test stand allows to measure the stiffness k and the damping factor c of ropes quite accurately. Some points remain to be clarified, but it does not question the results got with long samples if the 1% stiffness criterion is fulfilled.

This test stand can be operated either using a fixed sample length of 500 m, or for variable lengths of the sample from 5 to 500 m.

6.1 Operation with variable lengths of the sample

This is the way we used the test stand. Any sample of rope which abides by the stiffness ratio criterion detailed in §3 can be tested. The curve shown on Figure **33** gives the minimum length required as a function of the kL of the rope.

For example, a common steel rope with a diameter of 8 mm may have a kL around 5.10^6 N. In order to measure its characteristics with enough accuracy, the sample must have a length superior to 300 m. A common steel rope with a diameter of 16 mm is expected to have a kL equal to 13.10^6 N, hence a sample longer than 400 m must be used. A common fiber rope with a diameter of 8 mm is expected to have a kL equal to 2.10^6 N, hence a sample longer than about 200 m must be used.

Another limitation must be taken into consideration; the maximum load (rope's sample weight plus suspended mass) attached onto the cabin is limited to 1,5 T.

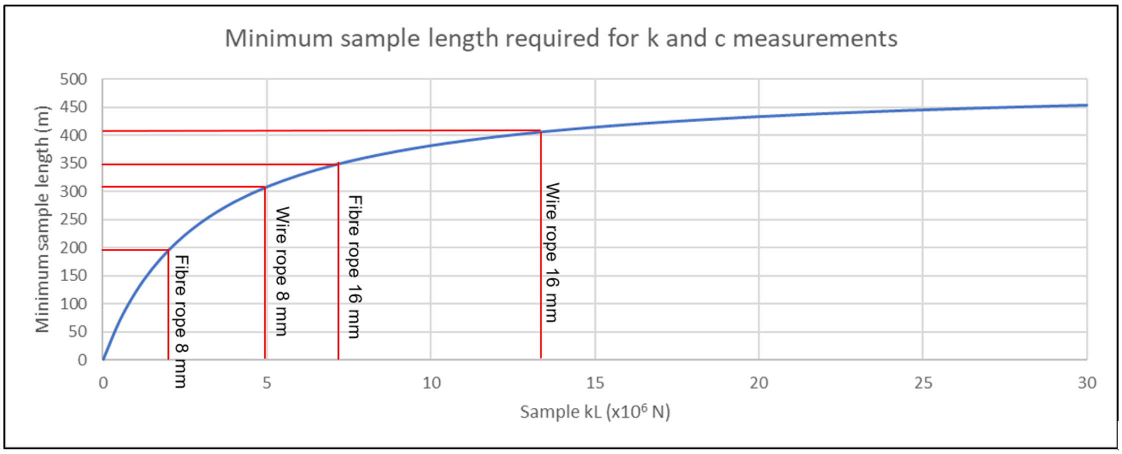

Figure 33: minimum sample length required according to the rope presumed stiffness

6.2 Operation with sample length of 500 m

The sample is hanged directly on the top structure. The 1% stiffness ratio between the sample stiffness and the top structure stiffness imposes that the maximum kL that can be tested is 415.10^6 N.

This would correspond to an 80 mm steel rope. However, such a rope could not be tested because this would require to hang a much heavier mass and to apply a higher initial load. The handling and the transfer of such masses would be tricky.

We can estimate that metallic ropes up to 30 mm and fiber ropes up to 40 mm can easily be tested on this bench. The stiffness ratio will be of about 0,2% which will make possible to perform accurate measurements of c and k at the length of 500 m (see §5.2).

Then c and k can be deduced for any rope length considering than cL and kL are rope constants.

7 Conclusions

The objective of the tests conducted until now was to determine the capabilities of the test stand and its limitations. From our test results, we can conclude that this test stand fulfils its function but can involve limitations regarding the sample length/stiffness, depending on the mode of operation.

Further tests can be conducted, mainly using the operation mode with variable sample lengths, to clarify the pending questions identified above.

The operation of the test stand with the 500 m sample length and within the 1% stiffness criterion will make it possible to quantify and then qualify ropes elastic behavior.

Further tests will allow to get better understanding of the rope's behavior, in particular:

+ how the damping can be influenced by the load intensity (safety factor)
+ evolution of the damping factor versus rope's diameter
+ quantification of ratio damping / critical damping versus rope's diameter, safety factor, …
+ how the rope's "bedding-in" influences the elastic behavior.

8 Acknowledgements

The authors would like to thank Director of ANDRA CMHM who made possible to use and temporarily transform the PX shaft into a wonderful test stand.

The authors also would like to thank Whitehill Manufacturing and Yale Cordage who supplied the fiber ropes, and also Verope AG who supplied most of the wire ropes which have been used for these tests.

The authors would also like to thank Laurent Bard, site engineer at DEP, who operated the test stand during the implementation of the tests.

9 References

[1] WEHKING, K.-H, VOGEL, W. and SCHULTZ, R. *Dämpfungsverhalten von Drahtseilen*. Fördern und Heben 49, 1999, pp.60-61.

[2] FEYRER, Klaus., *Wire Ropes, tension, endurance, reliability*. Springer, 2007, pp.82-85 & 95-99.

[3] HAMILTON, J., Vibration-based techniques for measuring elastic properties of ropes and the added mass of submerged objects, *Journal of atmospheric and oceanic technology*, 1999, vol. 17.

10 Authors introduction

Simon Varcin studied mechanical engineering at "Ecole des Mines" de Nancy and obtained his engineering degree in 2015. He first worked as research engineer in the field of automotive industry. He then joined DEP engineering in 2020 as calculation and research engineer.

Mathieu Fournier studied mechanical engineering at "Institut Supérieur de Mécanique de Paris – SUPMECA" and obtained his engineering degree in 2012. He immediatly joined DEP engineering as calculation and research engineer. He already took part in OIPEEC publications by Jean-Marc TEISSIER

Jean-Marc Teissier studied mechanical engineering at Grenoble University and is involved in the wire rope industry for more than 40 years. He is owner and managing director of DEP engineering since 1993. Thanks to collaboration with Roland Verreet DEP engineering moved toward research works related to wire ropes first and then to fiber ropes. He served as chairman of the scientific committee (2009 – 2017) and as President (2015 – 2019) of the OIPEEC.